Targeted ablation of the vitamin D receptor: An animal model of vitamin D-dependent rickets type II with alopecia

Yan Chun Li*, Alison E. Pirro*, Michael Amling†‡, Gunter Delling‡, Roland Baron†, Roderick Bronson§, and Marie B. Demay*¶

*Endocrine Unit, Massachusetts General Hospital and Harvard Medical School, 15 Fruit Street, Boston, MA 02114; †Department of Cell Biology, Yale University School of Medicine, 333 Cedar Street, New Haven, CT 06510; ‡Department of Bone Pathology, Hamburg University School of Medicine, Martinistrasse 52, 20246 Hamburg, Germany; and §Tufts University School of Veterinary Medicine and Human Nutrition Research Center, 711 Washington Street, Boston, MA 02111

ABSTRACT   Vitamin D, the major steroid hormone that controls mineral ion homeostasis, exerts its actions through the vitamin D receptor (VDR). The VDR is expressed in many tissues, including several tissues not thought to play a role in mineral metabolism. Studies in kindreds with VDR mutations (vitamin D-dependent rickets type II, VDDR II) have demonstrated hypocalcemia, hyperparathyroidism, rickets, and osteomalacia. Alopecia, which is not a feature of vitamin D deficiency, is seen in some kindreds. We have generated a mouse model of VDDR II by targeted ablation of the second zinc finger of the VDR DNA-binding domain. Despite known expression of the VDR in fetal life, homozygous mice are phenotypically normal at birth and demonstrate normal survival at least until 6 months. They become hypocalcemic at 21 days of age, at which time their parathyroid hormone (PTH) levels begin to rise. Hyperparathyroidism is accompanied by an increase in the size of the parathyroid gland as well as an increase in PTH mRNA levels. Rickets and osteomalacia are seen by day 35; however, as early as day 15, there is an expansion in the zone of hypertrophic chondrocytes in the growth plate. In contrast to animals made vitamin D deficient by dietary means, and like some patients with VDDR II, these mice develop progressive alopecia from the age of 4 weeks.

1,25-Dihydroxyvitamin D is the major steroid hormone that plays a role in mineral ion homeostasis. Its actions are thought to be mediated by a nuclear receptor, the vitamin D receptor (VDR), which heterodimerizes with the retinoid X receptor and interacts with specific DNA sequences on target genes. The VDR is evolutionarily well conserved and is expressed early in development in amphibians (1), mammals (2), and birds (3, 4). As well as being expressed in the intestine, the skeleton, and the parathyroid glands, the VDR is found in several tissues not thought to play a role in mineral ion homeostasis (5). Its precise functions in these tissues, as well as its developmental role, remain unclear.

Insights into the physiological actions of 1,25-dihydroxyvitamin D have been obtained from studies in vitamin D-deficient animals (6–10) as well as in humans with VDR mutations (11, 12). These investigations have demonstrated that 1,25-dihydroxyvitamin D plays an important role in intestinal calcium absorption and that animals lacking the active hormone or its nuclear receptor develop hypocalcemia, rickets, osteomalacia, and hyperparathyroidism. Although skin changes similar to psoriasis have been observed in vitamin D-deficient rats (13), the alopecia observed in some kindreds

with mutant VDRs has not been observed in vitamin D deficiency.

We have generated an animal model of vitamin D-dependent rickets type II (VDDR II) by targeted ablation of DNA encoding the second zinc finger of the DNA-binding domain of the VDR. The resultant animals are phenotypically normal at birth; however, they develop hypocalcemia, hyperparathyroidism, and alopecia within the first month of life.

MATERIALS AND METHODS

Generation of VDR Null Mice. The coding region of the rat VDR cDNA was reverse transcribed from ROS 17/2.8 cell mRNA and amplified by PCR to generate a probe for screening a 129/sv mouse genomic library (a kind gift of T. Doetschmann, University of Cincinnati, Cincinnati). Two overlapping clones containing the sequences encoding the second zinc finger (exon 3) to the termination codon (exon 9) of the mouse VDR gene were isolated after screening 1.2×10^6 plaque-forming units. A 5-kb *Xba*I fragment containing intronic sequences 5′ to exon 3 (including part of the polylinker of the phage arm) and a 3.5-kb *Xba*I fragment (including polylinker sequences from pUC 18) containing exons 4 and 5 of the receptor were subcloned into the *Xho*I and *Sal*I sites, respectively, of the plasmid pNeoTKXho (kindly provided by Zhoufeng Chen, California Institute of Technology, Pasadena, CA). This targeting vector was linearized with *Sal*I and introduced into J1 ES cells (kindly provided by En Li, Massachusetts General Hosptial, Boston) by electroporation. After 8 days of selection with G418 (250 μg/ml) and gancyclovir (2 μM), embryonic stem (ES) cell colonies were isolated and screened by Southern analysis for the presence of homologous recombinants. Out of 600 ES cell clones screened, 17 cell lines that had undergone homologous recombination were identified, 16 of which had a single copy of the neomycin resistance gene. Chimeric mice were produced by injecting the recombinant ES cells into 3.5-day C57BL/6J mouse blastocysts and reimplanting the blastocysts into pseudopregnant females. Chimeras derived from two independent ES cell clones gave germline transmission. Homozygous receptor ablated offspring from both clones showed identical phenotypes.

Animal Maintenance. Mice for generation of chimeras were obtained from Jackson Laboratories or Charles River Laboratories. All mice were kept in a virus- and parasite-free barrier facility. They were exposed to a 12-hr light/dark cycle and allowed free access to autoclaved water and chow. The Purina autoclavable rodent diet (5010) that they consumed contained

1% calcium, 0.67% phosphorus, and 4.4 units of vitamin D per gram.

Serum Chemistries. Parathyroid hormone levels were measured using a two-site assay for rat parathyroid hormone (PTH) (Corning). Ionized calcium levels were measured using a Ciba/Corning Ca^{2+}/pH analyzer. Serum phosphorus values were measured with a Cobas Mira analyzer (Roche).

Tissue Histology and *in Situ* Hybridization. The thyroid, parathyroids, trachea, and heart were removed en bloc from day-70 littermates to facilitate orientation of the specimens, permitting sectioning in the same plane. The specimens were fixed overnight in 4% formaldehyde in PBS, pH 7.2, processed, embedded in paraffin wax, and cut into 6-μm sections with a Leica RM 202 microtome. *In situ* hybridization was performed using an ^{35}S-UTP-labeled PTH cRNA probe synthesized from a linearized plasmid containing exons 2 and 3 as well as the corresponding intervening sequence of the rat PTH gene. The sense probe was synthesized using Sp6 RNA polymerase, and the antisense probe was synthesized using T7 RNA polymerase. For *in situ* hybridization (14), tissue sections were incubated at 65°C for 45 min. Following deparaffinization and rehydration, the sections were fixed again with 4% paraformaldehyde in PBS (15 min) and treated sequentially as follows: 10 μg/ml proteinase K in PBS (15 min); 4% paraformaldehyde in PBS (10 min); PBS wash (5 min); 0.2 N HCl (10 min); PBS wash (5 min); 0.1 M triethanolamine in 0.3% acetic anhydride (10 min); and PBS wash (5 min). The sections were then dehydrated with increasing concentrations of ethanol (70, 95, and 100%) and air-dried prior to hybridization.

Hybridization was carried out in a humidified chamber overnight at 55°C in 50% formamide/10 mM Tris·HCl, pH 7.6/1× Denhardt's solution/10% dextran sulfate/600 mM NaCl/0.25% SDS/200 μg/ml tRNA. After hybridization the sections were rinsed in 5× SSC at 50°C followed by a wash in 2× SSC/50% formamide at 50°C for 30 min. The slides were then treated with 10 μg/ml RNase A in TNE (10 mM Tris·HCl, pH 7.6/500 mM NaCl/1 mM EDTA) at 37°C for 30 min, and washed sequentially as follows: TNE (37°C, 10 min); 2× SSC (50°C, 20 min); 0.2× SSC, twice (50°C, 20 min). Following dehydration, the slides were air-dried and exposed to x-ray film for autoradiography. The slides were then dipped into NTB-2 emulsion (Kodak) and stored at 4°C for exposure of the emulsion. After development the slides were counter-stained with hematoxylin and eosin.

The femur, tibia, and fibula were isolated from 15- and 35-day-old mice and fixed in 4% formaldehyde for 18 hr at 4°C. After contact radiography (FaxitronContact, Faxitron, F.R.G.) and dehydration, the undecalcified bones were embedded in methylmethacrylate and 5-μm sections were prepared on a rotation microtome (Jung, Heidelberg, F.R.G.) as described (15). Sections were stained with toluidine blue, von Kossa, or Goldner trichrome and evaluated using a Zeiss microscope (Carl Zeiss).

RESULTS

VDR null ($-/-$) mice were generated by deleting a 5-kb fragment of genomic DNA encoding the second zinc finger of the receptor DNA-binding domain (Fig. 1). VDR ablated animals represented 22% of the offspring of heterozygous matings, suggesting that receptor ablation did not decrease embryonic survival. Reverse transcriptase (RT)-PCR demonstrated the presence of wild-type VDR transcripts in RNA isolated from the intestine and kidney of wild-type ($+/+$) and heterozygous ($+/-$) mice. A truncated RT-PCR product was generated by the $-/-$ RNA. Sequence analysis demonstrated
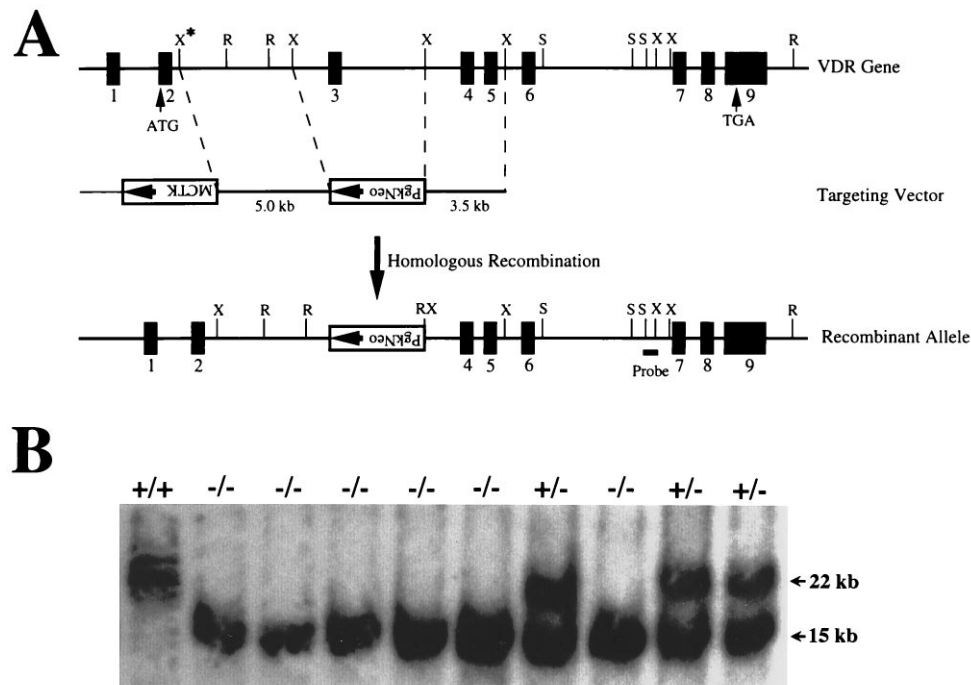

Fig. 1. Targeting strategy for VDR ablation. (*A*) Construction of targeting vector for VDR ablation. A schematic representation of the VDR gene is shown, based on the structure of the human gene and characterization of the sequences from exon 3 to exon 9 of the mouse gene. The exons are numbered and indicated by solid boxes. A partial restriction map is shown for the following enzymes: R, *Eco*RI; X, *Xba*I; S, *Sac*I. The *Xba*I site indicated by the asterisk was derived from the phage arm. A 5-kb *Xba*I fragment 5′ to exon 3 and a 3.5-kb *Xba*I fragment 3′ to exon 3 of the mouse VDR gene were used as the targeting sequences. The *Sac*I-*Xba*I fragment used as a probe for identifying homologous recombinants is indicated. (*B*) Genomic Southern analysis of tail DNA derived from offspring of heterozygous matings. The DNA was digested with *Eco*RI and hybridized with the external probe as indicated in *A*. The wild-type allele generates a 22-kb fragment, and the mutant allele resulting from homologous recombination produces a 15-kb fragment. Wild-type mice are indicated by $+/+$; heterozygous, by $+/-$; and homozygous receptor ablated mice, by $-/-$.

deletion of 131 bp of DNA encoding the second zinc finger, resulting in a frame shift followed by a termination codon 12 bp downstream. The −/− animals were indistinguishable from their +/+ and +/− littermates at birth; however, from 24 days of age, they failed to grow as rapidly as their +/+ and +/− littermates and weighed 10% less by 91 days of age (Fig. 2A). Their tibias and femurs were approximately 15% shorter than that of +/+ and +/− littermates. The +/− mice were phenotypically normal. Although the VDR −/− animals were normocalcemic until day 21, they became progressively hypocalcemic from that point, maintaining ionized calcium levels approximately 25% lower than that of their +/− and +/+ littermates (Fig. 2B). Concomitant with the development of hypocalcemia, a progressive increase in serum immunoreactive PTH levels was observed from day 21 in the −/− mice (Fig. 2C). Serum phosphorus levels were normal on day 16 (9.6 ± 0.2 versus 9.5 ± 0.9 mg/dl in the +/+ mice); however, correlating with the increase in immunoreactive PTH levels, the −/− mice became hypophosphatemic by day 21 (6.5 ± 0.5 vs. 10.5 ± 0.6 mg/dl). Examination of the parathyroid glands from day-70 mice revealed a marked increase in glandular size as well as in PTH mRNA content assessed by *in situ* hybridization (see Fig. 3). Based on the greatest diameter of the glands visualized on serial sections, and the number of sections in which the glands were visualized, the size of the parathyroid glands in the 70-day-old VDR ablated mice was increased more than 10-fold.

Contact radiography of the tibia at day 35 showed decreased cortical width along the diaphysis (arrowhead), as well as expansion and flaring of the growth plate (arrow), consistent with rickets (Fig. 4B). Histological analyses of the skeleton at this time showed decreased bone mineralization as assessed by von Kossa (Fig. 4D, mineral stains black) and Goldner trichrome (not shown) staining. Examination of the growth
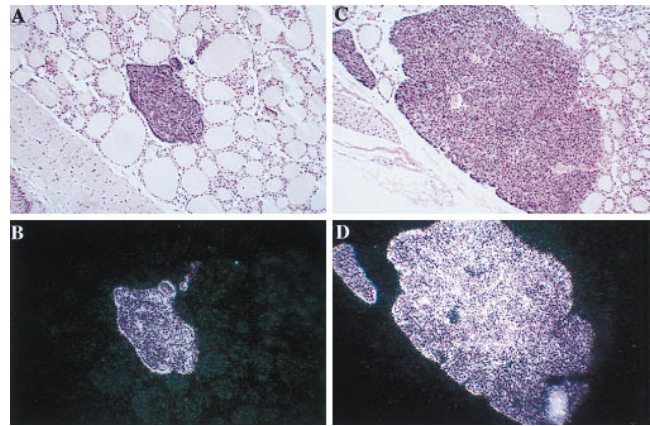

FIG. 3. *In situ* hybridization of parathyroid glands from VDR ablated mice with a rat PTH probe. (A) 25× magnification of hematoxylin and eosin counter-stained bright-field section of a parathyroid gland from 70-day-old +/+ mouse hybridized *in situ* for PTH mRNA. (B) Dark-field exposure of A. (C) 25× magnification of hematoxylin and eosin counter-stained bright-field section of a parathyroid gland from a 70-day-old −/− littermate hybridized *in situ* for PTH mRNA. (D) Dark-field exposure of C. No signal was observed using the sense probe.

plate at 35 days (Fig. 4F) revealed marked disorganization with an increase in vascularity (arrows), matrix (arrowhead), and zone of hypertrophic chondrocytes. Contact radiography and histology of the tibiae and vertebrae from day-15 littermates failed to show a defect in bone mineralization (not shown); however, examination of the growth plate at this time revealed a 15% increase in the number of hypertrophic chondrocytes per column (Fig. 4H, bracketed). The skeleton of the +/− animals was indistinguishable from that of the +/+ controls at both time points.
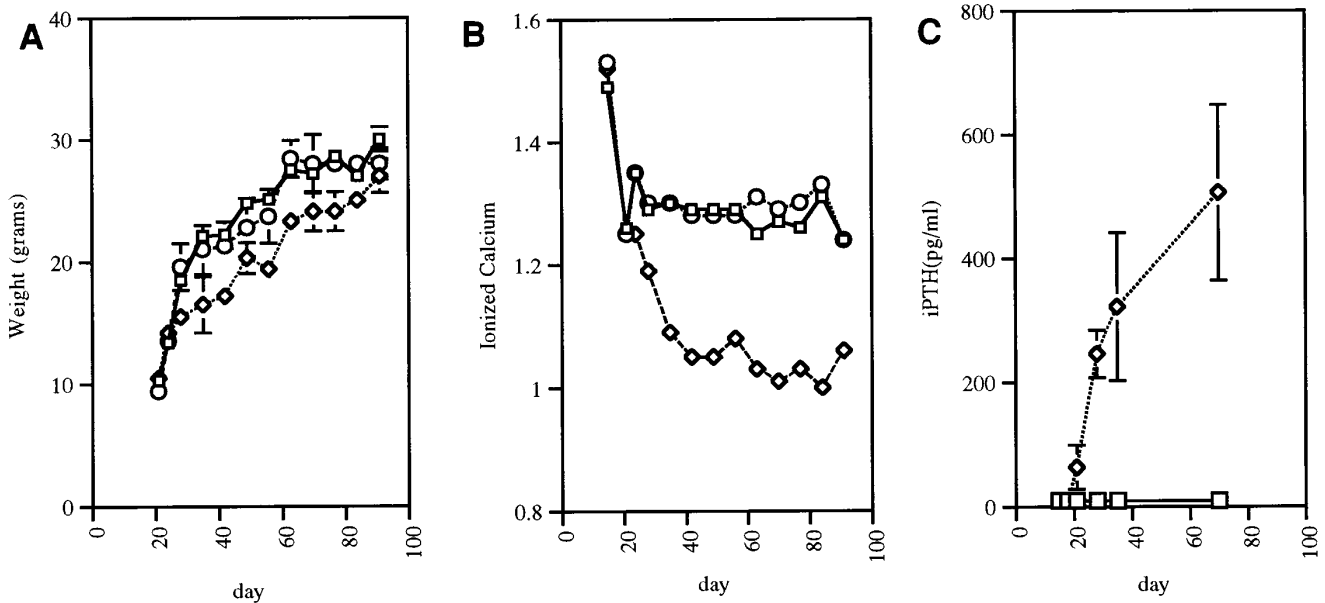

FIG. 2. Growth and serum chemistries of the VDR ablated mice. (A) Male mice of all three genotypes were weighed at weekly intervals from 2 to 13 weeks of age. The wild-type (squares) and heterozygous (circles) mice grow at a similar rate; however, the homozygous ablated (diamonds) mice gain weight more slowly after weaning (at 21 days of age). All values are based on three to five animals, and errors represent the SEM. Absence of error bars indicates points where the SEM is less than 0.6. The shape of the female weight curve is similar. (B) Ionized calcium measurements (in mmol/L, corrected for pH) were performed at weekly intervals from 2 to 13 weeks of age. Day 14 samples were obtained by cardiac puncture under isoflurane anesthesia. All other samples were obtained by tail nicking. The wild-type (squares) and heterozygous (circles) mice have similar levels, whereas the homozygous mice (diamonds) become hypocalcemic after weaning. All values represent the mean and SEM based on measurements in three to five mice. Absence of error bars indicates points where the SEM is less than 0.01. There was no sex difference in ionized calcium values. (C) Immunoreactive PTH values were measured using a rat PTH assay. iPTH values in the wild-type (squares) and heterozygous mice (data not shown) were less than 18 pg/ml at all stages. iPTH levels in the vitamin D receptor ablated mice (diamonds) were indistinguishable from those of their heterozygous and wild-type littermates at 15 and 19 days of age but by 21 days began to rise. All values are based on the mean and SEM of sera from three mice of the same genotype.
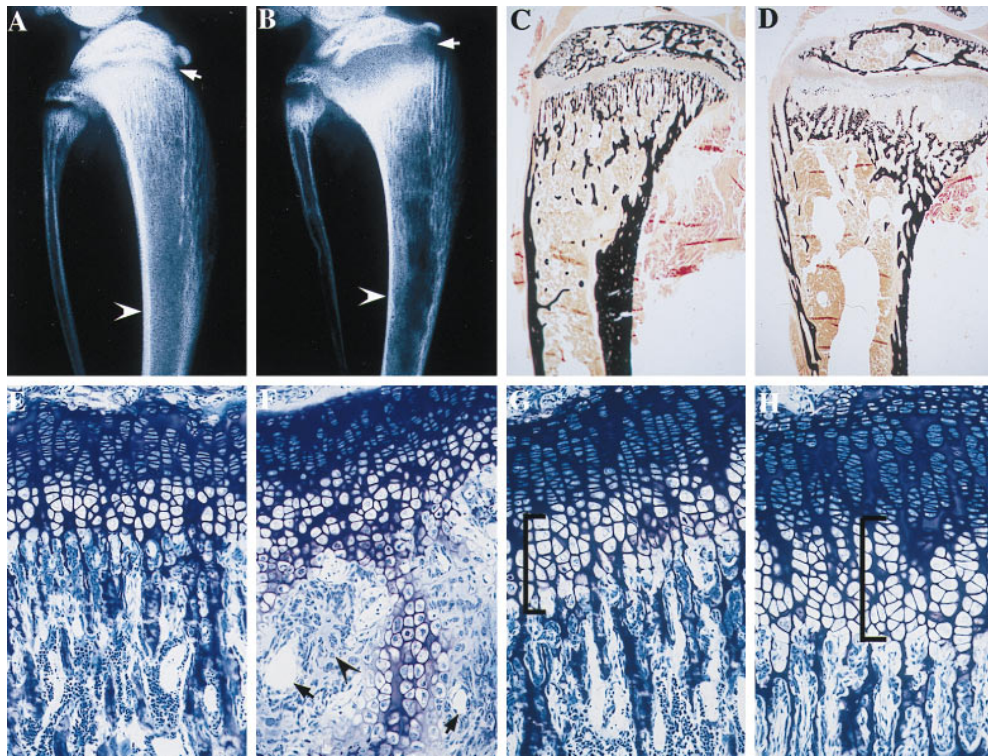
FIG. 4. Contact radiography and histology of the tibia of VDR ablated mice. (*A*) Contact x-ray of the tibia of a 35-day-old control mouse. (*B*) Contact x-ray of the tibia of a 35-day-old −/− littermate. (*C*) von Kossa stain of a nondemineralized section through the tibia of the 35-day-old control mouse. (*D*) von Kossa stain of a nondemineralized section through the tibia of a 35-day-old −/− littermate. (*E*) Toluidine blue section through the growth plate of the 35-day-old control mouse. (*F*) Toluidine blue section through the growth plate of the 35-day-old −/− littermate. (*G*) Toluidine blue section through the growth plate of a 15-day-old control mouse. (*H*) Toluidine blue section through the growth plate of a 15-day-old −/− littermate.

At the age of 4 weeks, the VDR −/− mice began to develop perioral and periorbital alopecia. As shown in Fig. 5, this hair loss progressed to involve the entire body over the next 3 months. Unlike kindreds with VDDR II, alopecia was uniformly observed in the −/− mice but progressed more rapidly in the females than in the males. Histological analyses of the skin of the VDR −/− mice revealed dilatation of the hair follicles with formation of dermal cysts.

Gross and microscopic autopsy of mice sacrificed at 70 days of age revealed only the pathological changes described above.

FIG. 5. Appearance of VDR ablated mice at 3.5 months of age. The genotypes of the mice, from left to right, are wild type, heterozygous, and homozygous ablated.

DISCUSSION

Although the VDR is widely expressed early during embryonic development, no major developmental abnormalities are observed in the VDR −/− mice or in humans with VDDR II. Like animals with dietary vitamin D deficiency and patients with VDDR II, the VDR−/− mice develop hypocalcemia postnatally. The time of onset of the hypocalcemia in the −/− mice is not unexpected in view of the observation that intestinal calcium absorption in rats occurs by a nonsaturable 1,25-dihydroxyvitamin D-independent mechanism the first 18 days of life (6). This nonsaturable component decreases until 35 days of age, gradually being replaced by a 1,25-dihydroxyvitamin D-dependent saturable component, which is detectable 18 days postpartum. It is of interest that a 1-week delay in weaning of the −/− pups (day 28) fails to prevent the growth retardation and the development of hypocalcemia. The increase in serum-immunoreactive PTH levels observed in the −/− mice correlates with the development of hypocalcemia; however, future studies will be required to address whether this increase is solely a consequence of the hypocalcemia, or whether the absence of antiproliferative (16) and transcription-repressing (17–19) effects of 1,25-dihydroxyvitamin D on the parathyroids also play a role.

Interestingly, the growth plate abnormalities we observed in the −/− mice antedate the development of disordered mineral ion homeostasis, which is observed as early as 15 days of age. These data suggest that, although the receptor-dependent actions of 1,25-dihydroxyvitamin D are not necessary for normal embryogenesis, they may play a role in the development and maturation of the growth plate, even in the setting of normal mineral ion homeostasis. By 35 days of age, however, both decreased mineralization of the bone and profound abnormalities in the growth plate are observed. Although the bone volume is not decreased in the −/− animals, there is a

15-fold increase in the amount of unmineralized bone (osteoid) by day 35. Calcein-labeling studies demonstrate that this is due to impaired mineral deposition.

Absence of functional VDRs has been shown to be the molecular basis for the disease, VDDR II. The majority of the characterized mutations in these kindreds involve point mutations in the DNA-binding domain of the receptor (reviewed in ref. 23). A few kindreds have been described with point mutations in the hormone-binding domain of the receptor; however, there is no discernible phenotypic difference between these individuals and those with DNA-binding domain mutations. The mutation that we have introduced deletes the second zinc finger of the DNA-binding domain and results in frame shift followed by premature termination codon. The apparent instability of the transcript generated by this mutation (as evidenced by its absence in the $+/-$ mice) is reminiscent of a human VDR mutation that results in a premature termination codon in the hormone-binding domain and is also thought to generate an unstable mRNA transcript (24). VDDR II is characterized by the development of hypocalcemia in infancy, accompanied by rickets, osteomalacia, and secondary hyperparathyroidism. Alopecia totalis is observed in some kindreds with VDDR II. The development of alopecia is felt by some investigators to be associated with a more profound 1,25-dihydroxyvitamin D resistance (20). Its presence in these kindreds parallels the development of rickets; however, alopecia totalis is not a feature of dietary vitamin D deficiency, nor is it observed in association with other hypocalcemic syndromes. Like the VDR $-/-$ mice, affected infants do not have alopecia at birth but, rather, develop progressive alopecia during infancy (12).

The VDR has been shown to be expressed in the outer root sheath keratinocytes and in the dermal papilla of the hair follicle (21). The development of secondary alopecia in both the $-/-$ mice and the VDDR II kindreds with alopecia suggests that the VDR plays a key role in the hair cycle rather than in primary hair growth. In a murine model, it has been shown that VDR expression in the hair follicle is increased during late anagen and catagen, correlating with decreased proliferation and increased differentiation of the keratinocytes (21). The effect of 1,25-dihydroxyvitamin D on keratinocyte differentiation and proliferation is supported by several *in vitro* studies (reviewed in ref. 22). Although keratinocytes are capable of synthesizing 1,25-dihydroxyvitamin D, suggesting an autocrine or paracrine regulation of the hair follicle, alopecia is not a feature of profound dietary vitamin D deficiency, nor is it observed in kindreds with vitamin D-dependent rickets type I who are unable to 1α hydroxylate vitamin D metabolites. Unlike some members of the nuclear receptor superfamily, the VDR has not been shown to have ligand-independent transcriptional activity; therefore, the development of alopecia in the presence of VDR deficiency and not ligand deficiency remains unexplained. Clarification of the molecular basis for the alopecia may reveal that the VDR has 1,25-dihydroxyvitamin D-independent effects on the hair follicle or that vitamin D metabolites present at high concentrations in the skin, even in the setting of severe vitamin D deficiency, play an important role in the regulation of the hair cycle.

1. Li, Y., Bergwitz, C., Jüppner, H. & Demay, M. (1997) *Endocrinology* **138,** 2347–2353.
2. Johnson, J. A., Grande, J. P., Roche, P. C. & Kumar, R. (1996) *J. Bone Miner. Res.* **11,** 56–61.
3. Elaroussi, M. A., Uhland-Smith, A., Hellwig, W. & DeLuca, H. F. (1994) *Biochim. Biophys. Acta* **1192,** 1–6.
4. Tuan, R. S. & Suyama, E. (1996) *J. Nutr.* **126,** 1308S–1316S.
5. Stumpf, W. E., Sar, M., Reid, F. A., Tanaka, Y. & DeLuca, H. F. (1979) *Science* **206,** 1188–1190.
6. Dostal, L. A. & Toverud, S. U. (1984) *Am. J. Physiol.* **246,** G528–G534.
7. Halloran, B. P. & DeLuca, H. F. (1981) *Arch. Biochem. Biophys.* **209,** 7–14.
8. Mathews, C. H. E., Brommage, R. & DeLuca, H. F. (1986) *Am. J. Physiol.* **250,** E725–E730.
9. Miller, S. C., Halloran, B. P., DeLuca, H. F. & Jee, W. S. S. (1983) *Calcif. Tissue Int.* **35,** 455–460.
10. Underwood, J. L. & DeLuca, H. F. (1984) *Am. J. Physiol.* **246,** E493–E498.
11. Balsan, S., Garabedian, M., Larchet, M., Gorski, A.-M., Cournot, G., Tau, C., Bourdeau, A., Silve, C. & Ricour, C. (1986) *J. Clin. Invest.* **77,** 1661–1667.
12. Beer, S., Tieder, M., Kohelet, D., Liberman, O. A., Vure, E., Bar-Joseph, G., Gabizon, D., Borochowitz, Z. U., Varon, M. & Modai, D. (1981) *Clin. Endocrinol.* **14,** 395–402.
13. Pavlovitch, J. H., Galoppin, L., Rizk, M., Didierjean, L. & Balsan, S. (1984) *Am. J. Physiol.* **247,** E228–E233.
14. Lee, K., Deeds, J. D. & Segre, G. V. (1995) *Endocrinology* **136,** 453–463.
15. Hahn, M., Vogel, M. & Delling, G. (1991) *Virchows Arch. A Pathol. Anat.* **418,** 1–7.
16. Ishimi, Y., Russell, J. & Sherwood, L. M. (1990) *J. Bone Miner. Res.* **5,** 755–760.
17. Silver, J., Russell, J. & Sherwood, L. M. (1985) *Proc. Natl. Acad. Sci. USA* **82,** 4270–4273.
18. Russell, J., Lettieri, D. & Sherwood, L. M. (1986) *Endocrinology* **119,** 2864–2866.
19. Silver, J., Naveh-Many, T., Mayer, H., Schmeizer, H. J. & Popovtzer, M. M. (1986) *J. Clin. Invest.* **78,** 1296–1301.
20. Marx, S. J., Bliziotes, M. M. & Nanes, M. (1986) *Clin. Endocrinol.* **25,** 373–381.
21. Reichrath, J., Schilli, M., Kerber, A., Bahmer, F. A., Czarnetzki, B. M. & Paus, R. (1994) *Br. J. Dermatol.* **131,** 477–482.
22. Bikle, D. D. & Pillai, S. (1993) *Endocr. Rev.* **14,** 3–19.
23. Malloy, P. J., Eccleshall, T. R., Gross, C., Van Maldergem, L., Bouillon, R. & Feldman, D. (1997). *J. Clin. Invest.* **99,** 297–304.
24. Ritchie, H. H., Hughes, M. R., Thompson, E. T., Malloy, P. J., Hochberg, Z., Feldman, D., Pike, J. W., & O'Malley, B. W. (1989) *Proc. Natl. Acad. Sci. USA* **86,** 9783–9787.